

Synthesis, Molecular Modeling Studies, and Selective Inhibitory Activity against Monoamine Oxidase of 1-Thiocarbamoyl-3,5-diaryl-4,5-dihydro-(1*H*)-pyrazole Derivatives

Franco Chimenti,[†] Elias Maccioni,[‡] Daniela Secci,^{*,†} Adriana Bolasco,[†] Paola Chimenti,[†] Arianna Granese,[†] Olivia Befani,[§] Paola Turini,[§] Stefano Alcaro,[#] Francesco Ortuso,[#] Roberto Cirilli,^{||} Francesco La Torre,^{||} Maria C. Cardia,[‡] and Simona Distinto[‡]

Dipartimento di Studi di Chimica e Tecnologia delle Sostanze Biologicamente Attive, Università degli Studi di Roma "La Sapienza", P.le A. Moro 5, 00185 Rome, Italy, Dipartimento di Scienze Biochimiche "A. Rossi Fanelli" and Centro di Biologia Molecolare del CNR Università degli Studi di Roma "La Sapienza", P.le A. Moro 5, 00185 Rome, Italy, Dipartimento di Scienze Farmaco Biologiche "Complesso Nini Barbieri", Università degli Studi di Catanzaro "Magna Graecia", 88021 Roccelletta di Borgia (CZ), Italy, Laboratorio di Chimica del Farmaco, Istituto Superiore di Sanità, Viale Regina Elena 299, 00161 Rome, Italy, and Dipartimento Farmaco Chimico Tecnologico, Università degli Studi di Cagliari, Via Ospedale 72, 09124 Cagliari, Italy

Received December 14, 2004

A novel series of 1-thiocarbamoyl-3,5-diaryl-4,5-dihydro-(1*H*)-pyrazole derivatives have been synthesized and investigated for the ability to inhibit selectively the activity of the A and B isoforms of monoamine oxidase (MAO). All the synthesized compounds show high activity against both the MAO-A and the MAO-B isoforms with K_i values between 27 and 4 nM and between 50 and 1.5 nM, respectively, except for a few derivatives whose inhibitory activity against MAO-B was in the micromolar range. Knowing that stereochemistry may be an important modulator of biological activity, we performed the semipreparative chromatographic enantioseparation of the most potent, selective, and chiral compounds. The separated enantiomers were then submitted to in vitro biological evaluation. The selectivity of the (–)-(S)-**1** enantiomer against MAO-B increases twice and a half, while the selectivity of the (–)-(S)-**4** enantiomer against MAO-A triples. Both the MAO-A and MAO-B isoforms respectively of the 1O5W and 1GOS models deposited in the Protein Data Bank were considered in the computational study. The docking study was carried out using several computational approaches with the aim of proposing possible binding modes of the MAO enantioselective compounds **1** and **4**.

Introduction

Monoamine oxidases (MAO) are widely distributed enzymes among mammals, plants, and prokaryotic and eukaryotic microorganisms that catalyze oxidatively amines to aldehydes. They are divided into two classes: aminoxidases containing copper(II) (EC, 1.4.3.6) and aminoxidases containing flavin (EC, 1.4.3.4).¹ The former aminoxidases contain copper(II) 2,4,5-trihydroxyphenylalanine quinone as cofactor (TPQ-Cu) and are inhibited by semicarbazide.² The latter aminoxidases contain flavin adenine dinucleotide (FAD) as cofactor and exist as two isoforms, MAO-A and MAO-B, which differ in substrate specificity and sensitivity to inhibitors. MAO-A preferentially deaminates serotonin and norepinephrine and is selectively inhibited by clorgyline, whereas MAO-B preferentially deaminates β -phenylethylamine and benzylamine and is selectively inhibited by L-deprenil.³ Dopamine, tyramine, and tryptamine are

common substrates for MAO-A and MAO-B. The two MAO isoforms are composed of 527 and 520 amino acids, respectively, with 70% of the amino acid identity.⁴ Both isoforms contain the FAD cofactor covalently linked to a cysteine residue in the active site.⁵ The catalytic mechanism of MAOs has been proposed with two different mechanisms: one radical, with the iminium cation as intermediate, and the other polar nucleophilic.⁶

MAOs are important in the metabolism of monoamine neurotransmitters, and as a result, MAO inhibitors (MAOI) are studied for the treatment of several psychiatric and neurological diseases. MAO-B inhibitors are coadjuvant in the treatment of Parkinson's disease⁷ and also Alzheimer's disease.⁸ MAO-A inhibitors are used as antidepressant and antianxiety drugs.⁹

In our previous studies, we focused attention on the importance of the presence of a 1-acetyl group in the pyrazoline nucleus for MAO inhibitory activity.^{10,11}

Other authors recently evaluated some 1-N-substituted thiocarbamoyl-3-phenyl-5-thienyl-2-pyrazolines and found MAO inhibitory activity in the 450–22 μ M range.¹²

Our knowledge of the chemistry and the MAO inhibitory activity of pyrazoline derivatives prompted us to study the influence of the substitution of the 1-acetyl group with a 1-unsubstituted thioamide one. The dipole

* To whom correspondence should be addressed. Phone and fax: +39 06 4991 3763. E-mail: daniela.secci@uniroma1.it.

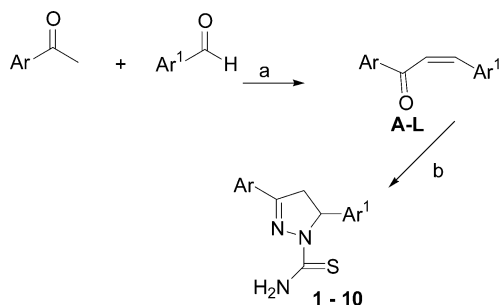
[†] Dipartimento di Studi di Chimica e Tecnologia delle Sostanze Biologicamente Attive, Università degli Studi di Roma "La Sapienza".

[‡] Università degli Studi di Cagliari.

[§] Dipartimento di Scienze Biochimiche "A. Rossi Fanelli" and Centro di Biologia Molecolare del CNR Università degli Studi di Roma "La Sapienza".

[#] Università degli Studi di Catanzaro "Magna Graecia".

^{||} Istituto Superiore di Sanità.

Scheme 1^a

^a Reagents and conditions: (a) KOH, EtOH, H₂O; (b) EtOH, thiosemicarbazide, KOH.

moments of many compounds indicate that the C=S group is more polarizable than the C=O group because of the larger kernel of electrons in the S atom.¹³ Therefore, the presence of an unsubstituted thiocarbamoyl group on the N1 position of the pyrazoline nucleus appears to be important for the inhibitory activity against both MAO isoforms and its importance is comparable with that of the acetyl group previously attested.^{10,11} For this reason we prepared and assayed for the MAO-A and -B inhibitory activities the new 1-thiocarbamoyl-3,5-diaryl-4,5-dihydro-(1*H*)-pyrazole derivatives **1–10**.

Owing to the presence of a chiral center at the C5 position of the pyrazole moiety and knowing that stereochemistry may be an important modulator of biological activity,¹⁴ we performed the semipreparative chromatographic enantioseparation of the most potent, selective, and active chiral compounds. To explain the selectivity of these enantiomers, a molecular modeling study was carried out using different docking approaches with the Protein Data Bank (PDB) enzymatic models of both MAO isoforms.

Chemistry

To verify the effects of structural modifications on both inhibition and selectivity toward MAO-A and MAO-B, the substituted 4,5-dihydro-(1*H*)-pyrazoles **1–10** have been synthesized. In particular, the influence, on the biological behavior, of the introduction of different aromatic rings in the 3 and 5 positions of the dihydro-(1*H*)-pyrazole nucleus has been investigated.

The starting 1,3-diaryl-2-propen-1-ones (chalcones) **A–L** have been synthesized according to literature methods.^{15–17}

The 1-thiocarbamoyl-3,5-diaryl-4,5-dihydro-(1*H*)-pyrazoles **1–10** were synthesized by reacting 1 equiv of chalcone, 2 equiv of thiosemicarbazide, and KOH in ethanol, as depicted in Scheme 1 and listed in Table 1.

By this method products **1–10** were synthesized with yields ranging from 48% to 58%. Crude products were crystallized from ethanol/isopropyl alcohol. The structures of the compounds were fully characterized by means of both mass spectrometry and ¹H NMR spectroscopy. In particular, the methylene protons and the methyne proton, in positions 4 and 5, respectively, of the dihydro-(1*H*)-pyrazole ring, give rise to a well-defined system of three double doublets, indicating not only the formation of the pyrazoline but also the exact position of the C=N double bond (Figure 1, compound **a**).

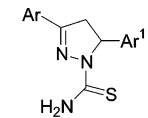
Direct Analytical and Semipreparative HPLC Enantioseparations of Samples 1 and 4. The enantiomers of racemic compounds **1** and **4** were separated on the analytical and the semipreparative scale by enantioselective HPLC on an amylose phenylcarbamate-based chiral stationary phase (CSP), the Chiralpak AD CSP.¹⁸ Baseline analytical enantioseparations (resolution factor *R*_s > 6) were achieved within 25 min by using binary mixture *n*-hexanes–ethanol 20:80 (v/v) or pure ethanol as mobile phases. The temperature column of 25 °C and flow rates of 1.0 and 0.5 mL min^{−1} were utilized. The sign of the optical rotation at a wavelength of 365 nm of the two enantiomers of **1** and **4** was determined by on-line polarimetric detection during HPLC enantioseparations on AD CSP. The second eluting enantiomers of **1** and **4** were dextrorotatory in both normal phase and polar organic conditions.

For the semipreparative runs, an amount of 5 mg of racemic sample was injected onto a 10 mm i.d. Chiralpak AD CSP by using pure ethanol as the mobile phase. After semipreparative separations, the collected fractions were analyzed by an analytical Chiralpak AD column (250 mm × 4.6 mm i.d.) to determine their enantiomeric excess (ee). Enantiomeric excess values greater than 99.0% and yields ranging from 70% to 90% for both enantiomers of compounds **1** and **4** were obtained.

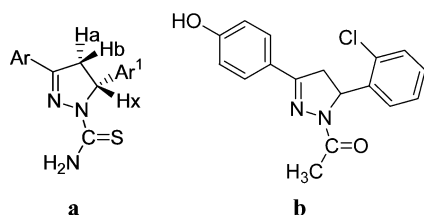
The specific rotations of the isolated enantiomers measured at 589 nm were as follows: (+)-**1**, [α]_D²³ +241 (c 0.10, CHCl₃); (−)-**1m**, [α]_D²³ −228 (c 0.10, CHCl₃); (+)-**4**, [α]_D²³ +208 (c 0.17, CHCl₃); (−)-**4**, [α]_D²³ −208 (c 0.19, CHCl₃). The (+)-enantiomer of the compounds examined was the more retained isomer on the polysaccharide-based AD CSP, and no inversion of elution order resulted in the scale-up procedure.

Stereochemical Characterization of the Enantiomers of 1 and 4. Taking into account the specific rotations of enantiomers of the structurally related chiral compound 1-acetyl-3-(4-hydroxyphenyl)-5-(2-chlorophenyl)-4,5-dihydro-(1*H*)-pyrazole (Figure 1, compound **b**), we used the sign of optical rotation as an experimental criterion for the configurational assignment of the stereogenic center C5 located at the pyrazole moiety.¹⁹ The assignment of the absolute configuration of enantiomers of compounds **1** and **4** could be empirically established according to their chiroptical and chromatographic properties. As above-reported, the on-line polarimetric measurements at 365 nm furnished a positive sign for the optical rotation for second eluting enantiomers of **1** and **4** both in ethanol and in *n*-hexanes–ethanol 20:80 (v/v). For the corresponding less retained enantiomers the sign of the rotations was inverted, as expected. Off-line polarimetric analysis at 589 nm indicated that the sign of rotation of polarized light was unmodified in chloroform solution (Figure 1, compound **b**).

Single-crystal X-ray diffraction analysis shows that the (+)-enantiomer of compound **b** has the absolute (*R*)-configuration.¹⁹ The (*R*)-enantiomer of compound **b** is dextrorotatory at 365 and 589 nm in both ethanol and chloroform solutions. The sign of optical rotation of (*R*)-**b** stereoisomer at 365 nm in *n*-hexanes–ethanol (70:30, v/v), online-monitored during chiral HPLC on AD CSP, was also +.

Table 1. Chemico Physical Properties of 1-Thiocarbamoyl-3,5-diaryl-4,5-dihydro-(1*H*)-pyrazole Derivatives **1–10**


compound	Ar	Ar ¹	mp (°C)	yield %	m/z
1			238-240	56	329
2			153-154	58	309
3			217-218	52	285
4			195-196	57	333
5			156-158	53	313
6			184-185	50	289
7			208-210	53	321
8			164-165	55	301
9			135-136	48	277
10			154-155	58	293

**Figure 1.** 1-Thiocarbamoyl-3,5-diaryl-4,5-dihydro-(1*H*)-pyrazole (**a**) and 1-acetyl-3-(4-hydroxyphenyl)-5-(2-chlorophenyl)-4,5-dihydro-(1*H*)-pyrazole (**b**).

Thus, with the assumption of a structural analogy between the studied compounds, the absolute configuration of enantiomers of **1** and **4** as (–)-(*S*) and (+)-(*R*) is straightforward.²⁰ Furthermore, of all analytes reported, **1**, **4**, and compound **b** exhibited the same sense chiral recognition mechanism and, consequently, the same enantiomer elution order on AD CSP in the presence of normal-phase *n*-hexanes–ethanol eluents, with preferential retention of the (+)-enantiomer. These data permit us to advance the hypothesis that the structurally related analytes investigated undergo same chiral recognition process on AD CSP and supports the presumption that the (+)-enantiomers of chiral analytes **1**, **4** and compound **b** possess the same absolute (*R*)-configuration.

Results and Discussion

All compounds were first evaluated for their ability to inhibit MAO in the presence of kynuramine as a substrate (Table 2). It is interesting to note that all compounds act through the reversible mode, as shown by dialysis performed over 24 h in a cold room against

a 0.1 M potassium phosphate buffer (pH 7.2) capable of restoring 90–100% of the activity of the enzyme. After a first assessment of their inhibitory ability on the MAO, the compounds were tested to determine their activity toward MAO-A and MAO-B selectively in the presence of the specific substrates, serotonin and benzylamine, respectively (Table 2).

From Table 2, which shows the MAO inhibition data along with the MAO inhibitory selectivity (SI B/A and A/B), it can be seen that all the synthesized compounds show high activity against both the MAO-A and the MAO-B isoforms with *K*_i values between 27 and 4 nM and between 50 and 1.5 nM, respectively, except for derivatives **3**, **4**, and **6** whose inhibitory activity was in the micromolar range against MAO-B.

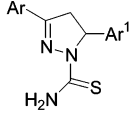
The 3,5-diphenyl derivatives **1**, **2**, **4**, and **5**, which bear a 4-chlorophenyl substituent in the 5 position, show high activity against both MAO-A and MAO-B but with opposite selectivity. In fact, derivative **1** with a methyl group in the Ar shows a selectivity toward MAO-B (SI-A/B) = 20.7), while derivative **4** with a 4-fluorine in the same position shows selectivity against MAO-A.

The derivatives **3** and **6**, 5-furyl substituted, exhibit selectivity for the MAO-A.

Compounds **7–10** have high activity against both isoforms, but for compounds **7** and **8** a little selectivity against MAO-B can be observed.

Furthermore, owing to the presence of a chiral center at the C5 position of the pyrazole moiety, semipreparative chromatographic enantioseparation of the most potent, selective, and active chiral compounds **1** (*K*_{iMAO-B} = 1.5 × 10^{−9}; SI = 20.7) and **4** (*K*_{iMAO-A} = 6.0 × 10^{−9}; SI = 166) was performed. The separated enantiomers

Table 2. Inhibitory Activities of 1-Thiocarbamoyl-3,5-diaryl-4,5-dihydro-(1*H*)-pyrazole Derivatives **1–10**^a

						
compound	Ar	Ar ¹	K _i M (±SD) MAO-A	K _i M (±SD) MAO-B	SI ^b B/A	SI ^c A/B
1			3.1 x 10 ⁻⁸ (±0.05)	1.5 x 10 ⁻⁹ (±0.02)	0.05	20.70
2			6.0 x 10 ⁻⁹ (±0.03)	1.0 x 10 ⁻⁸ (±0.07)	1.60	0.60
3			4.0 x 10 ⁻⁹ (±0.01)	1.7 x 10 ⁻⁷ (±0.02)	42.50	0.02
4			6.0 x 10 ⁻⁹ (±0.03)	1.0 x 10 ⁻⁶ (±0.04)	166.00	0.006
5			7.0 x 10 ⁻⁹ (±0.07)	5.0 x 10 ⁻⁸ (±0.06)	7.10	0.14
6			8.0 x 10 ⁻⁹ (±0.03)	3.7 x 10 ⁻⁷ (±0.01)	46.25	0.021
7			4.1 x 10 ⁻⁸ (±0.07)	6.0 x 10 ⁻⁹ (±0.01)	0.14	6.80
8			5.0 x 10 ⁻⁸ (±0.04)	1.0 x 10 ⁻⁸ (±0.02)	0.20	5.00
9			5.0 x 10 ⁻⁸ (±0.02)	2.0 x 10 ⁻⁸ (±0.05)	0.40	2.50
10			2.7 x 10 ⁻⁸ (±0.03)	5.0 x 10 ⁻⁸ (±0.01)	1.85	0.54

^a Data represent mean values of at least of three separate experiments. ^b SI: selectivity index = $K_{i(\text{MAO-B})}/K_{i(\text{MAO-A})}$. ^c SI: selectivity index = $K_{i(\text{MAO-A})}/K_{i(\text{MAO-B})}$.

Table 3. Inhibitory Activities of 1-Thiocarbamoyl-3,5-diaryl-4,5-dihydro-(1*H*)-pyrazole Derivatives **1–4**^a as Racemates and Single Enantiomers^a

compound	K _i M (±SD) MAO-A	K _i M (±SD) MAO-B	SI ^b B/A	SI ^c A/B
(±) 1	3.1 x 10 ⁻⁸ (±0.05)	1.5 x 10 ⁻⁹ (±0.02)	0.05	20.70
(-)-(S) 1	5.0 x 10 ⁻⁸ (±0.02)	1.0 x 10 ⁻⁹ (±0.01)	0.02	50.00
(+)-(R) 1	1.3 x 10 ⁻⁸ (±0.04)	2.7 x 10 ⁻⁹ (±0.07)	0.20	4.80
(±) 4	6.0 x 10 ⁻⁹ (±0.03)	1.0 x 10 ⁻⁶ (±0.04)	166.00	0.006
(-)-(S) 4	5.0 x 10 ⁻⁹ (±0.04)	2.4 x 10 ⁻⁶ (±0.01)	480.00	0.002
(+)-(R) 4	1.2 x 10 ⁻⁸ (±0.02)	1.4 x 10 ⁻⁶ (±0.05)	116.00	0.008

^a Data represent mean values of at least of three separate experiments. ^b SI: selectivity index = $K_{i(\text{MAO-B})}/K_{i(\text{MAO-A})}$. ^c SI: selectivity index = $K_{i(\text{MAO-A})}/K_{i(\text{MAO-B})}$.

were then submitted to in vitro biological evaluation (Table 3). From the results of these experiments it has been possible to point out a difference between the racemic mix and the individual enantiomers in inhibiting the two isoforms selectively. This is particularly evident in compound **1**, for which anti-MAO-B activity varies slightly, while selectivity increases twice and a half for the enantiomer (-)-(S), reaching 50.

For compound **4**, in the same way but for anti-MAO-A activity, selectivity triples for the enantiomer (-)-(S), reaching 480.

The computational work was carried out with the aim to rationalize the biological results obtained for each enantiomer of compounds **1** and **4**. It is worth noting that the main difference in the inhibition activity of these stereoisomers was found when the methyl of the first aromatic moiety is replaced by a fluorine atom. This

substitution was responsible for the remarkable differences in the inhibition activity mainly against MAO-B isoform, with a factor between 2400 and 519, respectively, for the (-)-(S) and (+)-(R) enantiomers of compounds **1** and **4**. The MAO-A effects of such substitutions were much lower with factors between 0 and 1, respectively. In the entire set of compounds, the highest substitution effect on the MAO-A inhibition is only 12.5 (data computed with racemate inhibition activities).

The catalytic cleft comparison of bovine MAO-A and MAO-B isoforms revealed a high level of identity.²¹ Between them only 1 of 12 residues is not conserved; Ile335 is replaced with Tyr326. The computational study started with the conformational analysis of (R)-isomers of compounds **1** and **4**. As expected for the position and nature of F and Me substitutions, the Monte Carlo (MC) search gave identical results in terms of conformational

Table 4. GLUE Binding Modes (BM) and Interaction Energies in kcal/mol

Complex	BM 1	BM 2	BM 3	BM 4	BM 5	BM 6	BM 7
[MAO-B-(S)-1]	-8.20	-5.13	-5.02	-4.78	-	-	-
[MAO-B-(R)-1]	-4.02	-3.78	-0.60	-0.60	-	-	-
[MAO-A-(S)-4]	-6.22	-5.50	-5.46	-5.31	-3.29	-2.55	-1.66
[MAO-A-(R)-4]	-8.22	-6.74	-6.13	-1.83	-0.71	-0.55	-
[MAO-A-(R)-1]	-5.74	-4.54	-4.09	-2.76	-	-	-
[MAO-A-(S)-1]	-6.08	-5.13	-4.65	-	-	-	-
[MAO-B-(R)-4]	-9.64	-3.99	-2.92	-0.55	-	-	-
[MAO-B-(S)-4]	-6.54	-6.51	-4.69	-3.08	-	-	-

distribution in both compounds: two conformers within 12.5 kcal/mol above the global minimum. The main differences were due to two thiourea moiety rotamers attached to the pyrazole N1 atom (data not shown).

Both conformers obtained in the MC search and their Z mirrored images ((S)-stereoisomers) were used for an intensive series of docking experiments with the MAO-A and MAO-B isoforms corresponding to 1O5W and 1GOS PDB models. The docking experiments were started following a computational approach reported in our recent publications.²² The MOLINE method²³ was carried out after the enzyme pretreatment (see Experimental Section), fixing the Cartesian origin of the XYZ axes onto the FAD N5 atom and varying the resolution and the compression factor. Unlike our previous results obtained with coumarine derivatives,²² we found binding modes of compounds **1** and **4** in the enzymatic cleft of both isoforms only in a few cases. So we decided to use GLIDE²⁴ as an alternative docking method. Using no energy filtering control and a box size including all catalytic residues, with this approach it was possible to generate 10 configurations of each compound in the enzymatic clefts. Unfortunately, the unique OPLS-AA force field implemented in GLIDE, version 1.8, generated a tetrahedral unrealistic geometry in the sp² carbon of the thiourea. Probably as a consequence of this poor parametrization, the GLIDE scoring functions related to this ensemble gave a weak correlation with experimental data. However, we used the 80 binding modes (10 for each ligand complex) as a starting point for further energetic analysis based on multim minimization procedures in different conditions with MacroModel, version 7.2.²⁵ (see Experimental Section), again with no interesting results. Therefore, similar experiments were carried out using the GLUE flexible docking approach included in the GRID suite²⁶ considering all probes related to the chemical groups of compounds **1** and **4** (see Experimental Section). Multiple binding modes (BM) varying from 3 to 7 were detected with this approach. Despite the fact that the conformational treatment of the thiourea moiety was better, the interaction energies did not give an acceptable correlation with the experimental data, not even in this case (Table 4).

The reason for such unsatisfactory results was attributed mainly to a missing explicit solvent in the above models. In a recent publication, Binda et al.²⁷ highlighted the importance of structural water in the catalytic region close to the FAD cofactor also in the

presence of noncovalent ligands complexed to the MAO-B isoform. To take into account this issue and to consider the reciprocal induced fit effects adequately, the lowest interaction energy configurations BM1 (Table 4) obtained by the GLUE docking simulations were submitted to the GROMACS²⁸ molecular dynamic approach. After standard building procedures, with the aim of minimizing van der Waals contact with the solvent, the eight models were submitted to preliminary energy optimization with no constraints, followed by a dynamic conformational assessment of the water molecules, the ligand, and the FAD. After a short molecular dynamics (MD) run, we observed free binding interaction energies converted into affinity constants in good agreement with the experimental data. Moreover, similar to a reported analysis of MAO-B binding modes,²² the distance between each docked ligand and FAD N5 was considered as a geometrical descriptor possibly related to inhibition data (see Experimental Section). As a matter of fact, the GLUE–GROMACS docking configurations showed interesting correlations with experimental data from the point of view of energy and geometry (Table 5).

Details of the binding modes obtained in the GLUE–GROMACS, sorted by the experimental inhibition constants of Table 3, are reported in Figures 2 and 3.

The binding mode of the most active MAO-B inhibitor (S)-**1** observed at the end of the MD simulation was stabilized in the Ar¹ moiety portion by stacking interactions with Tyr398 and Tyr435. Electrostatic contributions were found between the Cl atom and the side chain OH of Tyr188. The thiourea moiety showed hydrophobic contact with Tyr60 and a weak hydrogen bond with a water molecule. The Ar moiety, located far from enzyme cofactor, established an interaction with the hydrophobic core defined by Phe168, Leu171, Cys172, Ile199, and Tyr326 (Figure 2a).

In the same enzymatic cleft, its enantiomer (R)-**1** was similarly oriented as far as regards the aromatic ring positions. No Ar¹ stacking was observed, but the van der Waals contacts were evident with the isoalloxazine FAD ring, Tyr398, and Tyr435. Moreover, with this residue the thiourea S atom established a first hydrogen bond and a second one with a water molecule close to Cys172. Similar to its enantiomer, the Ar moiety (R)-**1** interacted with the same cluster of hydrophobic residues (Figure 2b).

The binding mode of (S)-**4** in the MAO-A cleft was characterized by a totally different pattern with respect to the two docking results reported above. The fluori-

Table 5. GLUE–GROMACS Binding Mode Analysis

Complex	K _i M (±SD)	Theoretical Affinity constant	Ligand–FAD distance (Å)
[MAO-B/(S)-1]	1.0 x 10 ⁻⁹ (±0.01)	5.14 x 10 ⁻⁹	7.80
[MAO-B/(R)-1]	2.7 x 10 ⁻⁹ (±0.07)	2.21 x 10 ⁻⁹	9.50
[MAO-A/(S)-4]	5.0 x 10 ⁻⁹ (±0.04)	2.04 x 10 ⁻¹¹	9.35
[MAO-A/(R)-4]	1.2 x 10 ⁻⁸ (±0.02)	3.25 x 10 ⁻⁸	8.47
[MAO-A/(R)-1]	1.3 x 10 ⁻⁸ (±0.04)	1.45 x 10 ⁻⁸	9.40
[MAO-A/(S)-1]	5.0 x 10 ⁻⁸ (±0.02)	3.50 x 10 ⁻⁸	7.79
[MAO-B/(R)-4]	1.4 x 10 ⁻⁶ (±0.05)	6.27 x 10 ⁻⁸	9.84
[MAO-B/(S)-4]	2.4 x 10 ⁻⁶ (±0.01)	2.26 x 10 ⁻⁷	13.64

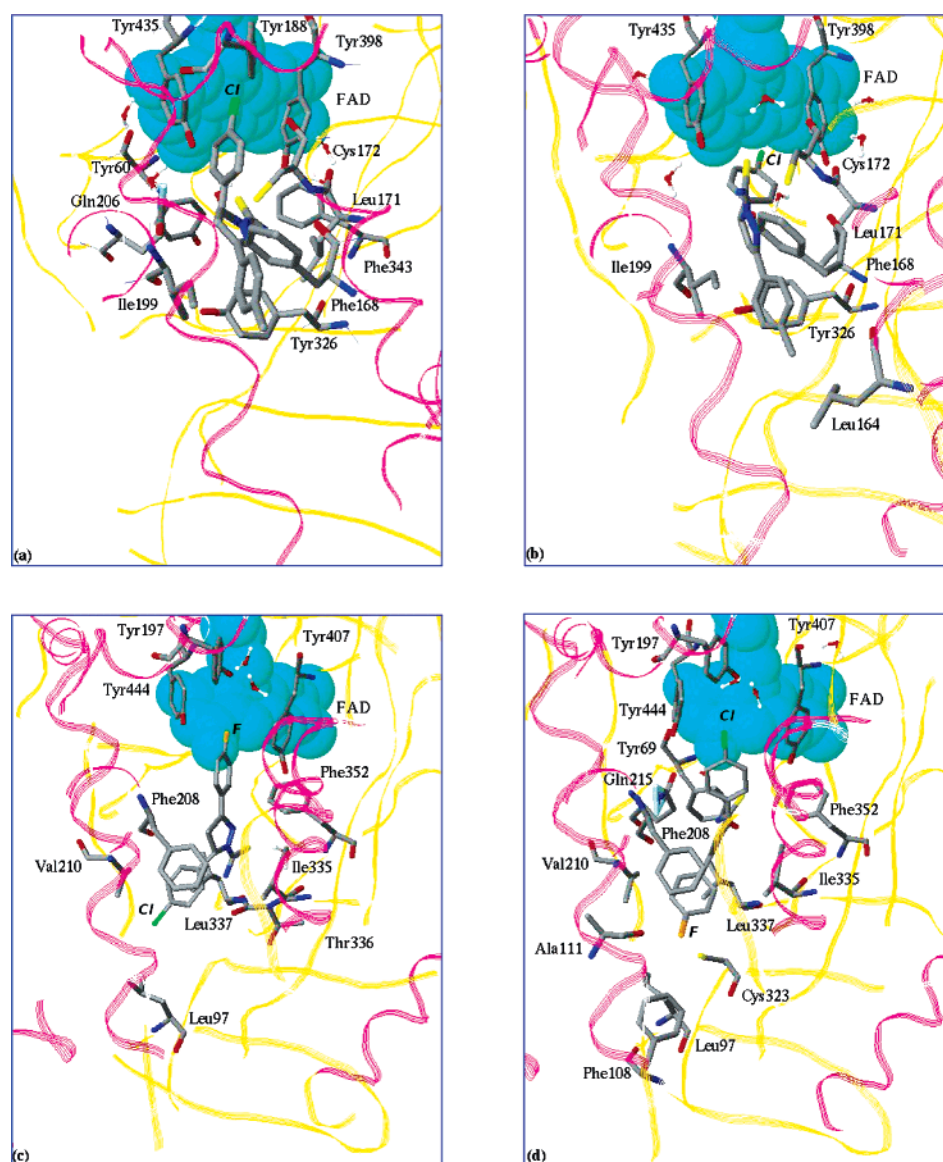


Figure 2. GLUE–GROMACS binding configurations of complexes [MAO-B/(S)-1] (a), [MAO-B/(R)-1] (b), [MAO-A/(S)-4] (c), and [MAO-A/(R)-4] (d). The inhibitors are displayed in bold polytubes, cofactor in cyan CPK, and residues of the enzymatic clefts in polytube models. For clarity, all other residues are depicted in structure colored ribbon and hydrogen atoms are omitted. Water molecules are displayed as balls and stick models.

nated Ar moiety was positioned close to the cofactor in a hydrophobic cavity delimited by Tyr197, Phe352, Tyr407, and Tyr444. An electrostatic attraction between F and a water molecule stabilized this binding mode. Moreover, two intermolecular hydrogen bonds were

detected: one between the thiourea S atom and a water molecule close to Phe352 and Ile335 and another between the amide hydrogen and the Thr336 backbone. The Ar¹ is located in a hydrophobic core delimited by Leu97, Phe208, Val210, and Leu337 (Figure 2c).

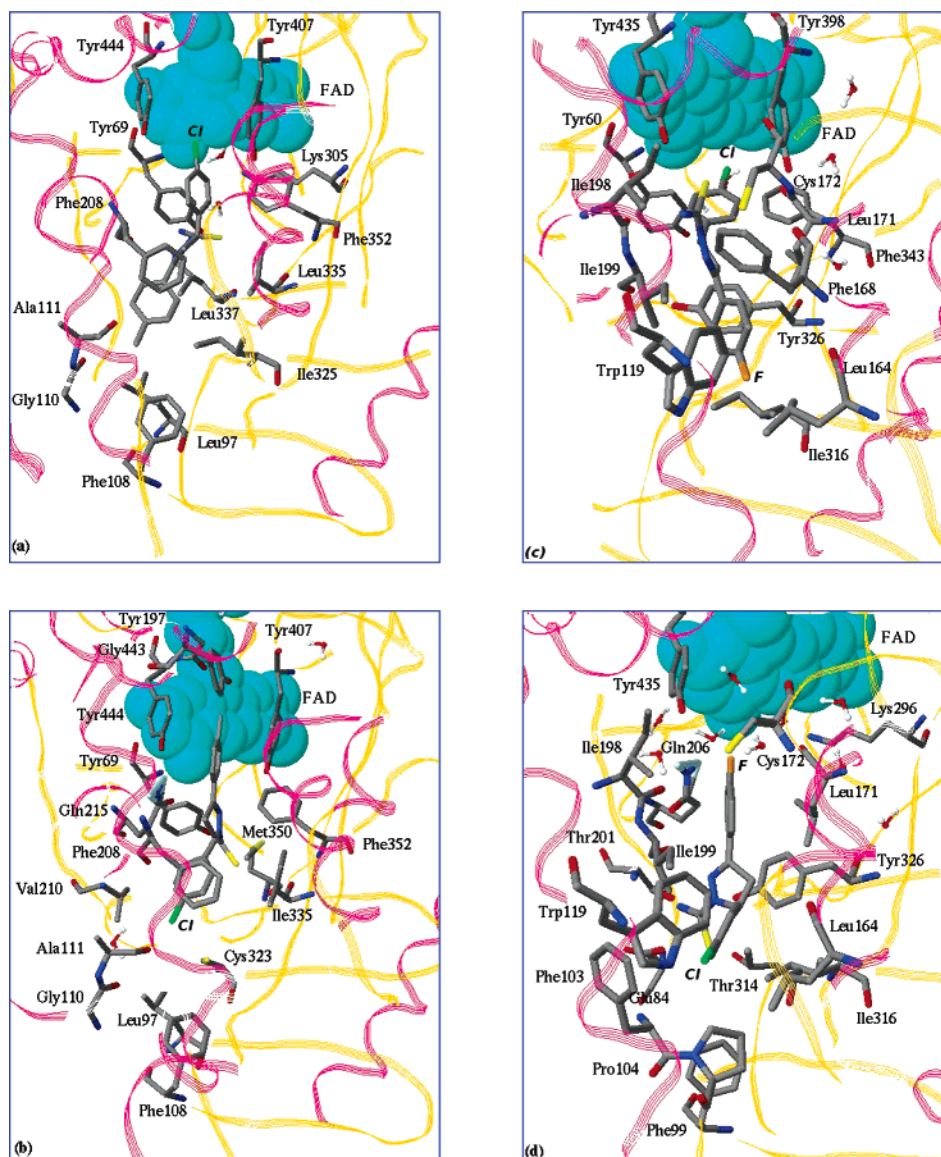


Figure 3. GLUE-GROMACS binding configurations of complexes [MAO-A/(*R*)-1] (a), [MAO-A/(*S*)-1] (b), [MAO-B/(*R*)-4] (c), and [MAO-B/(*S*)-4] (d). The inhibitors are displayed in bold polytubes, cofactor in cyan CPK and residues of the enzymatic clefts in polytube models. For clarity all other residues are depicted in structure colored ribbon, and hydrogen atoms are omitted. Water molecules are displayed as balls and stick models.

Conversely, in the MAO-A cleft its enantiomer (*R*)-4 displayed a binding pattern relatively similar to that of (*R*)-1 in the isoform B of the enzyme, with the Ar moiety far from FAD in a nonpolar region delimited by Leu97, Phe108, Ala111, Phe208, Val210, Cys323, Ile335, and Leu337. The Ar¹ group established van der Waals contacts without stacking with Tyr407 and Tyr444, while its Cl atom gave an attractive electrostatic interaction with a water molecule close to Tyr197 and to a second solvent molecule. FAD contacts with the ligand were basically hindered by these water molecules (Figure 2d).

Similar to (*R*)-4, (*R*)-1 also showed the same Ar¹ position in the MAO-A enzymatic cleft. The Ar moiety, and in particular its methyl group, established van der Waals interaction with nonpolar residues such as Leu97, Phe108, Gly110, Ala111, and Ile325 and a partial stacking with Phe208. The thiourea gave a similar interaction with Tyr69, Leu337, and Phe352. Notably in this binding mode, according to Binda's observations,²⁷ the FAD N5 was hindered by a hydrogen

bond interaction with a bridge water molecule with Lys305 (Figure 3a).

Its enantiomer (*S*)-1 in the same MAO-A enzymatic cleft displayed the opposite pattern, with its Ar moiety stacking with Tyr407 and Tyr444 and other contacts with FAD, Tyr197, and Gly443. On the other side of the ligand, Ar¹ recognized a hydrophobic cleft with Leu97, Phe108, Phe208, Val210, and Cys323. Its Cl atom established electrostatic interactions with a water molecule close to Gly110 and Ala111. Those two residues, quite far from FAD, seemed to prevent a better ligand-cofactor interaction (Figure 3b).

The binding mode of (*R*)-4 within the MAO-B enzyme was characterized by a repulsion interaction of the ligand Cl atom and FAD N5, which probably prevents closer contacts with the cofactor as shown by the distance analysis in Table 5. Other contacts of the Ar¹ moiety were detected with the hydrophobic residues Tyr60, Phe343, Tyr398, and Tyr435. Similar to the recognition of (*R*)-1, a hydrogen bond of S thiourea with Tyr435 was observed as well as the interaction of the

Ar ring in a hydrophobic area delimited by Trp119, Leu164, Phe168, Leu171, Ile199, Ile316, and Tyr326 (Figure 3c).

Finally, its enantiomer (*S*)-**1** interacts with MAO-B in a region significantly far from FAD compared to previous docking results. The cofactor was actually hindered by several water molecules. According to Binda's observation,²⁷ one of these molecules showed the same hydrogen bond network with FAD N5 and Lys296. Ar¹ established mainly hydrophobic interactions with residues already encountered in other recognition patterns, such as Trp119, Leu164, Ile199, Ile316, and others relatively far from the catalytic region, such as Phe103, Pro104, and Phe99. The Ar¹ F atom was hydrogen-bonded to the SH of Cys172, and the rest of the moiety established van der Waals contacts with Leu171, Ile198, Gln206, and Tyr435. Other interactions were also displayed between the thiourea moiety and Glu84, Thr201, and Thr314 (Figure 3d).

As a result of an analysis of the binding modes found at the end of the MD simulation carried out with best scoring GLUE configurations, it was possible to draw the following conclusions. Two main kinds of binding modes were detected on the basis of the relative positions of Ar and Ar¹ with respect to FAD. They were unrelated to the degree of inhibition. In agreement with previous studies,²² the inhibition activity of the **1** and **4** stereoisomers on both enzyme isoforms was regulated by their ability to establish close and productive interactions with FAD. In particular, the competition with water molecules, especially those capable of interacting with FAD N5 with the support of Lys305 (MAO-A) or Lys296 (MAO-B),²⁷ seemed to play an additional role in the inhibition activity. In fact the investigation of this last issue required the adoption of computational simulation with an explicit model of solvation.

We are focusing this computational work onto a larger library of (1*H*)-pyrazole derivatives with the aim of finding more predictive and general models for reversible and selective MAO inhibitors.

Experimental Section

Chemistry. Melting points are uncorrected and were determined on a Reichert Kofler thermopan apparatus. ¹H NMR spectra were recorded on a Bruker AMX (300 MHz) using tetramethylsilane (TMS) as internal standard and DMSO or CDCl₃ as solvents (chemical shifts in δ values, *J* in Hz). Electron ionization (EI) mass spectra were obtained by a Fisons QMD 1000 mass spectrometer (70 eV, 200 μ A, ion source temperature of 200 °C). The samples were introduced directly into the ion source. Elemental analyses for C, H, and N were performed on a Perkin-Elmer 240 B microanalyzer, and the analytical results were within $\pm 0.4\%$ of the theoretical values.

Preparation of 1-Thiocarbamoyl-3-(4-methylphenyl)-5-(4-chlorophenyl)-4,5-dihydropyrazole (1). A mixture of 1.80 g (0.007 mol) of 1-(4-methylphenyl)-3-(4-chlorophenyl)-2-propen-1-one and 1.27 g (0.014 mol) of thiosemicarbazide is refluxed in ethanol (70 mL) under vigorous stirring. After complete dissolution of the reactants, a solution of 0.78 g (0.014 mol) of KOH in ethanol (70 mL) is added dropwise. The solution is refluxed for a further 6 h, allowed to cool, and stirred overnight. A precipitate is formed, which is filtered off and crystallized from ethanol/isopropyl alcohol to give **1** as a pure product.

According to the same procedure, compounds **2–10** were synthesized.

Chromatographic (HPLC) Resolution of Racemic Samples 1 and 4. Chiral HPLC of **1** and **4** was performed by stainless steel Chiralcel OD columns (250 mm \times 4.6 mm i.d. and 250 mm \times 10 mm i.d.) (Daicel Chemical Industries, Tokyo, Japan). HPLC-grade solvents were supplied by Carlo Erba (Milan, Italy).

Chiral HPLC was performed using a Waters (Milford, MA) 510 pump equipped with a Rheodyne (Cotati, CA) injector, a 1 mL sample loop, an HPLC Perkin-Elmer (Norwalk, CT) oven, and a Waters model 996 diode array detector (DAD).

The sign of the optical rotation of the two enantiomers of **1** and **4** was measured on-line at wavelengths of 365 and 589 nm by a Perkin-Elmer polarimeter model 241 equipped with Hg/Na lamps and a 40 μ L flow cell. The system was kept at a constant temperature of 25 °C. The output signal was acquired and processed by Millenium 2010 software.

Biochemistry. All chemicals were commercial reagents of analytical grade and were used without purification. Bovine brain mitochondria were isolated according to Basford.²⁹ In all experiments the AO activities of the beef brain mitochondria were determined by a fluorimetric method, according to Matsumoto et al.³⁰ using kinuramine as a substrate at four different final concentrations ranging from 5 μ M to 0.1 mM. Briefly, the incubation mixtures contained 0.1 mL of 0.25 M potassium phosphate buffer (pH 7.4), mitochondria (6 mg/mL), and drug solutions with final concentration ranging from 0 to 10⁻³ μ M.

The solutions were incubated at 38 °C for 30 min. Addition of perchloric acid ended the reaction. The samples were centrifuged at 10000g for 5 min, and the supernatant was added to 2.7 mL of 0.1 N NaOH. The pyrazole derivatives were dissolved in dimethyl sulfoxide (DMSO), added to the reaction mixture from 0 to 10⁻³ μ M. To study the inhibition of pyrazole derivatives on the activities of both MAO-A and MAO-B separately, the mitochondrial fractions were preincubated at 38 °C for 30 min before adding the specific inhibitors (0.5 μ M L-deprenyl to estimate MAO A activity and 0.05 μ M clorgyline to assay the isoform B), considering that MAO-A is irreversibly inhibited by a low concentration of clorgyline but is unaffected by a low concentration of L-deprenyl, which is used in the MAO-B form. Fluorimetric measurements were recorded with a Perkin-Elmer LS 50B spectrofluorimeter. The protein concentration was determined according to Bradford.³¹ The results are reported in Table 2. Dixon plots were used to estimate the inhibition constant (*K_i*) of the inhibitors (data reported in Table 3). The data are the mean values of three or more experiments performed in duplicate.

Molecular Modeling. The Monte Carlo search of compounds **1** and **4** was carried out using the (*R*)-stereoisomer. A thousand conformations were generated randomizing the rotatable bonds of the common skeleton with an AMBER* united atom force field and GB/SA water implicit solvation as implemented in MacroModel, version 7.2.²⁵

Following the computational work of our recent communications,^{11,22} the Protein Data Bank MAO-B crystallographic model 1GOS³² was considered for the docking experiments. As regards the MAO-A, a crystallographic model of the rat isoform was reported recently in the PDB with the code 1O5W.³³ Both PDB models were obtained as adducts with two similar compounds covalently linked to the FAD N5 nitrogen.

The 1GOS model is related to the MAO-B isoform. The difference between human and bovine sequence at the catalytic site is related to one mutation; Ile199 is replaced with Phe199.

The comparison of human and rat MAO-A enzymes is respectively 90% as a global identity and 100% as a binding site.³³ So 1GOS and 1O5W models were considered in the computational study.

Pretreatment of the original PDB structures consisted of a 48 kcal/mol constrained energy minimization of those residues out of a radius of 15 Å from the N5 of the isoalloxazine ring in order to restore the natural planarity of the isoalloxazine FAD ring and relax the active site amino acids. In the resulting energy minimum structures, the covalent ligands (pargyline for 1GOS and clorgyline for 1O5W) were removed and used

as receptor models. This was performed with the force field AMBER* united atom notation and GB/SA water implicit model of solvation as implemented in MacroModel, version 7.2.²⁵

The MOLINE computational approach required as receptor and ligand input data, respectively, the pretreated enzyme models and the two conformations obtained in the MC search of the inhibitors. The docking experiments were carried out with the same AMBER* united atom force field considered in the simulations above. According to a recently reported²² similar case study, both the MOLINE grid resolution GR and the van der Waals compression factor χ were systematically varied. Two different dielectric constants respectively fixed at 4 (to mimic conditions similar to an "average" protein medium) and 80 (water environment) were tried in the docking experiments.

According to the GLIDE²⁴ approach, both pretreated enzyme models were submitted to map calculations using a box of about 110 000 Å³ centered on the FAD N5 atom. Flexible docking of the four ligands was done by generating a maximum number of 1000 configurations, saving the 10 lowest energy ones and submitting them to the multim minimization procedures as follows. We considered the MMFF, AMBER* united atoms and all-atom force fields. OPLS* did not work for missing parameters related to the FAD phosphate moiety. For solvation models, we considered two different dielectric constants and the water implicit GB/SA solvation model.²⁵ Three different constraint conditions were systematically studied: full relaxing (no constraints), protein backbone fixed with a 200 kJ mol⁻¹ Å⁻¹ force constant on each atom, and a shell of free atoms up to 15 Å from the FAD N5 with the remaining atoms kept constrained as above. The interaction energy of all complexes was computed according to the MOLINE method²³ and converted to average state equations. Globally, $8 \times 10 \times 3 \times 3 \times 3 = 2160$ conformations were energy-minimized at the above conditions.

Molecular interaction fields required by the GLUE program were precalculated by GRID using the standard probes OH2 and H. Specific probes related to the chemical structures of **1** and **4** were C3, C1=, N2, N=, F, CL, and O. This last probe was used to mimic the thiourea S atom, not available in the GLUE probe list. In the generation of the GRID maps, a cube box of 10 000 Å³ was centered on the FAD N5 atom using the original PDB models without their covalent ligands. The flexibility of the inhibitors was considered, allowing free rotations of all rotatable bonds of compounds **1** and **4**. The lowest interaction energy configurations of each complex were submitted to GROMACS calculations.

The force field considered in the GROMACS calculations was the ffgmx force field with the SPC explicit model of solvation.³⁴ GROMACS specific modules editconf and genbox were used to add water molecules within a box edge of minimum 10 Å from the enzyme complex. The module genion allowed the neutralization of the models by adding three Cl⁻ and four Na⁺ counterions to the MAO-A and MAO-B complexes, respectively. The PRODRG service tool available on the Internet was used for a quick setup of the non-protein section of the eight complexes.³⁵ Preliminary minimization was done using 500 iterations of the steepest descents algorithm with an energy convergence criterion fixed at 1000 kJ mol⁻¹ nm⁻¹. The particle mesh Ewald (PME) method was used to treat the electrostatic term.³⁶ Dynamic conformational assessment of non-protein atoms was carried out by Berendsen's temperature and pressure coupling method³⁷ for 2 ps at 300 K with a time step of 2 fs. The linear constraints solver algorithm (LINCS) was adopted for all atoms, preventing bond distortions as suggested for time steps larger than 1 fs.³⁸ The g_lie GROMACS utility was used to estimate the free-binding interaction energy of each enzyme-inhibitor complex (FBIE) using final conformations of the 2 ps molecular dynamics run. Theoretical affinity constants (K_a) were derived according to the equation $RT \ln K_a = \text{FBIE}$, where R is the gas constant and T the room temperature set to 300 K. The same conformations were submitted to geometrical analysis considering the

distance between the ligand centers of mass and the FAD N5 atom. A longer simulation up to 20 ps revealed no significant changes in this geometrical descriptor after 2 ps in all complexes.

All calculations were done by a Linux cluster of 5 Intel Xeon dual processors at 3.2 GHz with 2 Gb of RAM. Graphic manipulations and analysis of the docking experiments were performed by the Maestro Graphical User Interface, version 4.1.012, for Linux operating systems.²⁵ Jmol, version 10, was used for creating Figures 2 and 3.³⁹

Acknowledgment. This work was supported by grants from MURST. We also acknowledge Mr. Anton Gerada, a professional translator and Fellow of the Institute of Translation and Interpreting of London and Member of AIIC (Association Internationale des Interprètes de Conférences, Geneva), for the revision of the manuscript.

Supporting Information Available: ¹H NMR, IR spectral data, and elemental analysis results of derivatives **1–10**. This material is available free of charge via the Internet at <http://pubs.acs.org>.

References

- (1) Singer, T. P.; Von Korff, R. W.; Murphy, D. L. In *Monoamine Oxidase: Structure, Function and Altered Functions*; Academic: New York, 1979.
- (2) Mure, M.; Mills, S. A.; Klinman, J. P. Catalytic mechanism of the Topa quinone containing copper amine oxidases. *Biochemistry* **2002**, *41* (30), 9269–9278.
- (3) (a) Johnston, J. P. Some observations upon a new inhibitor of monoamine oxidase in brain tissue. *Biochem. Pharmacol.* **1968**, *17*, 1285–1297. (b) Knoll, J.; Magyar, K. Puzzling pharmacological effects of monoamine oxidase [MAO] inhibitors. *Adv. Biochem. Psychopharmacol.* **1972**, *5*, 393–408.
- (4) Bach, A. W.; Lan, N. C.; Johnson, D. L.; Abell, C. W.; Bembenek, M. E.; Kwan, S. W.; Seeburg, P. H.; Shih, J. C. cDNA cloning of human liver monoamine oxidase A and B: molecular basis of differences in enzymatic properties. *Proc. Natl. Acad. Sci. U.S.A.* **1988**, *85*, 4934–4938.
- (5) Wouters, J. Structural aspects of monoamine oxidase and its reversible inhibition. *Curr. Med. Chem.* **1998**, *5*, 137–162.
- (6) (a) Walker, M. C.; Edmondson, D. E. Structure–activity relationships in the oxidation of benzylamine analogues by bovine liver mitochondrial monoamine oxidase B. *Biochemistry* **1994**, *33* (23), 7088–7098. (b) Miller, J. R.; Edmondson, D. E. Structure–activity relationships in the oxidation of para-substituted benzylamine analogues by recombinant human liver monoamine oxidase A. *Biochemistry* **1999**, *38* (41), 13670–13683. (c) Silverman, R. B.; Hoffman, S. J.; Catus, W. B. A mechanism for mitochondrial monoamine oxidase catalyzed amine oxidation. *J. Am. Chem. Soc.* **1980**, *102* (23), 7126–7128. (d) Kim, J. M.; Bogdan, M. A.; Mariano, P. S. Mechanistic analysis of the 3-methylflavin-promoted oxidative deamination of benzylamine. A potential model for monoamine oxidase catalysis. *J. Am. Chem. Soc.* **1993**, *115* (23), 10591–10595. (e) Lu, X.; Rodriguez, M.; Gu, W.; Silverman, R. B. Inactivation of mitochondrial monoamine oxidase B by methylthio-substituted benzylamines. *Bioorg. Med. Chem.* **2003**, *11* (20), 4423–4430.
- (7) Cesura, A. M.; Pletscher, A. The new generation of monoamine oxidase inhibitors. *Prog. Drug Res.* **1992**, *38*, 171–297.
- (8) Saura, J.; Luque, J. M.; Cesura, A. M.; Da Prada, M.; Chan-Palay, V.; Huber, G.; Löffler, J.; Richards, J. Increased monoamine oxidase B activity in plaque-associated astrocytes of Alzheimer brains revealed by quantitative enzyme radioautography. *Neuroscience* **1994**, *62* (1), 15–30.
- (9) Amrein, R.; Martin, J. R.; Cameron, A. M. Moclobemide in patients with dementia and depression. *Adv. Neurol.* **1999**, *80*, 509–519.
- (10) Chimenti, F.; Bolasco, A.; Manna, F.; Secci, D.; Chimenti, P.; Befani, O.; Turini, P.; Giovannini, V.; Mondovi, B.; Cirilli, R.; La Torre, F. Synthesis and selective inhibitory activity against MAO of 1-acetyl-3,5-diphenyl-4,5-dihydro-(1H)-pyrazole derivatives. *J. Med. Chem.* **2004**, *47* (8), 2071–2074.
- (11) Manna, F.; Chimenti, F.; Bolasco, A.; Secci, D.; Bizzarri, B.; Befani, O.; Turini, P.; Mondovi, B.; Alcaro, S.; Tafi, A. Inhibition of amine oxidases activity by 1-acetyl-3,5-diphenyl-4,5-dihydro-(1H)-pyrazole derivatives. *Bioorg. Med. Chem. Lett.* **2002**, *12*, 3629–3633.
- (12) Gokhan, N.; Yesilada, A.; Ucar, G.; Erol, K.; Bilgin, A. A. 1-N-substituted thiocarbonyl-3-phenyl-5-thienyl-2-pyrazolines: Synthesis and evaluation as MAO inhibitors. *Arch. Pharm. (Weinheim, Ger.)* **2003**, *336*, 362–371.

- (13) Walter, W.; Voss, J. In *The Chemistry of Amides*; Zabicky, J., Ed.; Wiley and Sons Ltd.: London, 1970; Chapter 8, pp 385–415.
- (14) Takasaki, W.; Yamamura, M.; Nozaki, A.; Nitani, T.; Sasahara, K.; Itoh, K.; Tanaka, Y. Stereoselective pharmacokinetics of RS-8359, a selective and reversible MAO-A inhibitor, by species-dependent drug-metabolizing enzymes. *Chirality* **2005**, *17*, 135–141.
- (15) (a) Drake, N. L.; Allen, P. *Org. Synth. Collect.* J. Wiley and Sons, Inc.: London, 1948; 1, pp 77–78. (b) Kohler, E. P.; Chadwell, H. M. *Org. Synth. Collect.* J. Wiley and Sons, Inc.: London, 1948; 1, pp 78–79.
- (16) Nielsen, A. T.; Houlihan, W. J. *The Aldol Condensation in Organic Reactions*; Wiley and Sons: New York, London, Sydney, 1968; Vol. 16.
- (17) Bonsignore, L.; Cabiddu, S.; Maccioni, A.; Marongiu, E. Synthesis and separation of geometrical isomers of arylacrylonaphthones. *Gazz. Chim. Ital.* **1976**, *106*, 617–624.
- (18) Yashima, E.; Yamamoto, C.; Okamoto, Y. Polysaccharide-based chiral LC columns. *Synlett* **1998**, 344–360.
- (19) Cirilli, R.; Ferretti, R.; Gallinella, B.; Turchetto, L.; Bolasco, A.; Secci, D.; Chimenti, P.; Pierini, M.; Fares, V.; Befani, O.; La Torre, F. Enantiomers of C-5-chiral 1-acetyl-3,5-diphenyl-4,5-dihydro-(1*H*)-pyrazole derivatives: Analytical and semipreparative HPLC separation, chiroptical properties, absolute configuration, and inhibitory activity against monoamine oxidase. *Chirality* **2004**, *16*, 625–636.
- (20) Roussel, C.; Del Rio, A.; Pierrot-Sanders, J.; Piras, P.; Vanthuyne, N. Chiral liquid chromatography contribution to the determination of the absolute configuration of enantiomers. *J. Chromatogr., A* **2004**, *1037* (1–2), 311–328.
- (21) Abell, C. W.; Kwan, S. W. Molecular characterization of monoamine oxidases A and B. *Prog. Nucleic Acid Res. Mol. Biol.* **2000**, *65*, 129–156.
- (22) Chimenti, F.; Secci, D.; Bolasco, A.; Chimenti, P.; Granese, A.; Befani, O.; Turini, P.; Alcaro, S.; Ortuso, F. Inhibition of monoamine oxidases by coumarin-3-acyl derivatives: biological activity and computational study. *Bioorg. Med. Chem. Lett.* **2004**, *14*, 3697–3703.
- (23) Alcaro, S.; Gasparrini, F.; Incani, O.; Mecucci, S.; Misiti, D.; Pierini, M.; Villani, C. A. Quasi-flexible automatic docking processing for studying stereoselective recognition mechanisms. Part I. Protocol validation. *J. Comput. Chem.* **2000**, *21*, 515–530.
- (24) Eldridge, M. D.; Murray, C. W.; Auton, T. R.; Paolini, G. V.; Mee, R. P. Empirical scoring functions 1. The development of a fast empirical scoring function to estimate the binding affinity of ligands in receptor complexes. *J. Comput.-Aided Mol. Des.* **1997**, *11*, 425–445.
- (25) (a) *MacroModel*, version 7.2; Schrödinger Inc.: Portland, OR, 1998–2001. (b) Mohamadi, F.; Richards, N. G. J.; Guida, W. C.; Liskamp, R.; Lipton, M.; Caufield, C.; Chang, G.; Hendrickson, T.; Still, W. C. MacroModel, an integrated software system for modeling organic and bioorganic molecules using molecular mechanics. *J. Comput. Chem.* **1990**, *11*, 440–467.
- (26) (a) *GRID*, version 22a; Molecular Discovery Ltd.: West Way House, Elms Parade, Oxford, England. (b) Goodford, P. J. A computational procedure for determining energetically favorable binding sites on biologically important macromolecules. *J. Med. Chem.* **1985**, *28*, 849–857.
- (27) Binda, C.; Li, M.; Hubálek, F.; Restelli, N.; Edmondson, D. E.; Mattevi, A. Insights into the mode of inhibition of human mitochondrial monoamine oxidase B from high-resolution crystal structures. *Proc. Natl. Acad. Sci. U.S.A.* **2003**, *100*, 9750–9755.
- (28) (a) Berendsen, H. J. C.; van der Spoel, D.; van Drunen, R. GROMACS: A message-passing parallel molecular dynamics implementation. *Comput. Phys. Commun.* **1995**, *91*, 43–56. (b) Lindahl, E.; Hess, B.; van der Spoel, D. GROMACS 3.0: A package for molecular simulation and trajectory analysis. *J. Mol. Model.* **2001**, *7*, 306–317.
- (29) Basford, R. E. Preparation and properties of brain mitochondria. *Methods Enzymol.* **1967**, *10*, 96–101.
- (30) Matsumoto, T.; Suzuki, O.; Furuta, T.; Asai, M.; Kurokawa, Y.; Rimura, Y.; Katsumata, Y.; Takahashi, I. A sensitive fluorometric assay for serum monoamine oxidase with kynuramine as substrate. *Clin. Biochem.* **1985**, *18*, 126–129.
- (31) Bradford, M. M. A rapid and sensitive method for the quantitation of microgram quantities of protein utilizing the principle of protein–dye binding. *Anal. Biochem.* **1976**, *72*, 248–254.
- (32) Binda, C.; Newton-Vinson, P.; Hubálek, F.; Edmondson, D. E.; Mattevi, A. Structure of human monoamine oxidase B, a drug target for the treatment of neurological disorders. *Nat. Struct. Biol.* **2002**, *9*, 22–26.
- (33) Ma, J.; Yoshimura, M.; Yamashita, E.; Nakagawa, A.; Ito, A.; Tsukihara, T. Structure of rat monoamine oxidase A and its specific recognitions for substrates and inhibitors. *J. Mol. Biol.* **2004**, *338*, 103–114.
- (34) Berendsen, H. J.; Postma, J. P. M.; van Gunsteren, W. F.; Hermans, J. Interaction Models for Water in Relation to Protein Hydration. In *Intermolecular Forces*; Pullman, B., Ed.; D. Reidel Publishing Co.: Dordrecht, The Netherlands, 1981; pp 331–342.
- (35) (a) URL: <http://davapc1.bioch.dundee.ac.uk/programs/prodrg>. (b) Schuettelkopf, A. W.; van Aalten, D. M. F. PRODRG, a tool for highthroughput crystallography of protein–ligand complexes. *Acta Crystallogr.* **2004**, *D60*, 1355–1363.
- (36) (a) Darden, T.; York, D.; Pedersen, L. Particle mesh Ewald: An N -log(N) method for Ewald sums in large systems. *J. Chem. Phys.* **1993**, *98*, 10089–10092. (b) Essmann, U.; Perera, L.; Berkowitz, M. L.; Darden, T.; Lee, H.; Pedersen, L. A smooth particle mesh ewald potential. *J. Chem. Phys.* **1995**, *103*, 8577–8592.
- (37) Berendsen, H. J. C.; Postma, J. P. M.; van Gunsteren, W. F.; Di Nola, A.; Haak, J. R. Molecular dynamics with coupling to an external bath. *J. Chem. Phys.* **1984**, *81*, 3584–3590.
- (38) Hess, B.; Bekker, H.; Berendsen, H.; Fraaije, J. LINCS: A linear constraint solver for molecular simulations. *J. Comput. Chem.* **1997**, *18*, 1463–1472.
- (39) *Jmol*, version 10; <http://jmol.sourceforge.net>.

JM040903T